PHOTONICS Research

212-kHz-linewidth, transform-limited pulses from a single-frequency Q-switched fiber laser based on a few-layer Bi_2Se_3 saturable absorber

Weiwei Li, Jinhai Zou, Yizhong Huang, Kaijie Wang, Tuanjie Du, Shuisen Jiang, and Zhengqian Luo*

Department of Electronic Engineering, Xiamen University, Xiamen 361005, China
**Corresponding author: zqluo@xmu.edu.cn*

Received 18 July 2018; accepted 24 July 2018; posted 25 July 2018 (Doc. ID 338121); published 27 August 2018

Conventional *Q*-switched fiber lasers operating at multi-longitudinal-mode oscillation usually suffer from self-mode-locking-induced temporal instability, relatively strong noise, and low coherence. Here, we address the challenge through demonstrating, for the first time, to the best of our knowledge, a single-longitudinal-mode (SLM) Er-doped fiber (EDF) laser passively *Q*-switched by a few-layer Bi_2Se_3 saturable absorber (SA). The Bi_2Se_3 SA prepared by the liquid-phase exfoliation method shows a modulation depth of ~5% and saturation optical intensity of 1.8 MW/cm^2. A section of 1-m unpumped EDF together with a 0.06-nm-bandwidth fiber Bragg grating is used as an ultra-narrow autotracking filter to realize SLM oscillation. Stable SLM *Q*-switching operation at 1.55 μm is successfully achieved with the spectral linewidth as narrow as 212 kHz and the pulse duration of 2.54 μs, manifesting near-transform-limited pulses with a time-bandwidth product of 0.53. In particular, we found that the SLM *Q*-switching possesses the higher signal-to-noise ratios of 62 dB (optical) and 48 dB (radio frequency), exhibiting its advantages of low noise and high stability. Such an SLM *Q*-switched fiber laser could gain great interest for some applications in coherent detection, coherent optical communications, and high-sensitivity optical sensing.

OCIS codes: (140.3510) Lasers, fiber; (140.3540) Lasers, Q-switched.

https://doi.org/10.1364/PRJ.6.000C29

1. INTRODUCTION

The pursuit for *Q*-switched fiber lasers arises from their versatile applications to remote sensing, range finding, medicine, laser processing, and telecommunications [1]. At present, most *Q*-switched fiber lasers operate at multi-longitudinal-mode (MLM) oscillation. In contrast, single-longitudinal-mode (SLM) *Q*-switched fiber laser sources with the ultra-narrow linewidth and high peak power could be more intriguing in some special applications, such as Doppler lidar, differential absorption lidar, coherent optical communications, and high-resolution optical sensing [2–4]. Therefore, there is strong motivation to exploit SML *Q*-switched fiber lasers.

Q-switching operation of fiber lasers can be achieved either actively or passively. Active *Q*-switching usually requires an acoustic-optic or electro-optic modulator in the laser cavity, which will inevitably increase the cost and complexity of the laser system. In contrast, passively *Q*-switched fiber lasers based on saturable absorbers (SAs) possess the attractive advantages of compactness, simplicity, and flexibility in design [1]. To date, considerable efforts have been made toward passively *Q*-switched fiber lasers using different kinds of SAs [5–10], such as transition metal-doped crystals [5,6], semiconductor SA mirrors [7,8], carbon nanotubes [9,10], and two-dimensional (2D) materials [e.g., graphene, transition-metal dichalcogenides (TMDs), topological insulators (TIs), black phosphorus (BP), MXenes]. As the most focused SA materials currently, 2D materials have been under extensive studies in recent years [1,11–43]. For example, graphene/graphene oxide-based SAs have been exploited to successfully produce pulses in fiber lasers from 0.8 μm to 3 μm [11–21]. Since 2014, pulsed fiber lasers using TMDs [22–33] or BP [34–40] SAs have also been reported from the visible to infrared region. Comparatively, TIs (e.g., Bi_2Se_3) are of special interest owing to their excellent advantages of broadband saturable absorption and ultra-high modulation depth (up to 98%), which was uncovered and identified in 2012 [44]. Since then, TI-based passively *Q*-switched or mode-locked fiber lasers have been widely demonstrated [44–61]. Zhao *et al.* first used Bi_2Se_3 as an effective SA for the passive mode locking of an erbium-doped fiber laser (EDFL) [44,45]. Shortly afterwards, they reported

a Bi_2Se_3-based [46] and a Bi_2Te_3-based [47] Q-switched EDFL, respectively. Large pulse energy up to 1.5 μJ and tunable Q-switching operation from 1510.9 nm to 1589.1 nm were obtained [47], revealing its great potential as a Q-switcher for laser pulse generation. Our research group achieved the passively Q-switched pulses in the 0.63 μm, 1 μm, and 2 μm regions, respectively, by inserting a Bi_2Se_3 SA into Pr^{3+}-doped [51], Yb^{3+}-doped [52], and Tm^{3+}-doped fiber lasers [53]. In 2015, Li *et al.* further extended the operating waveband of TI-based SAs to 3 μm by inserting a Bi_2Te_3-based SA into a linear-cavity Ho^{3+}-doped ZBLAN fiber laser [54]. These results reveal the broadband saturable absorption of TI-based SAs.

Although the rapid development of the Q-switched fiber lasers based on TI-based SAs has been made, most of the works mentioned above focused on time-domain performance but ignored other aspects (e.g., spectral linewidth) of them. Moreover, it should be especially noted that all of them operated at MLM oscillation. The effects of self-mode-locking and mode-hopping [62,63] in MLM Q-switched fiber lasers could deteriorate the Q-switching operation and degrade the stability of the output laser pulses. On the contrary, if one realizes narrow-linewidth SLM Q-switching operation in a fiber laser, the overall performance of Q-switched pulses could be significantly improved with excellent stability, low noise, and high coherence.

In this paper, we report the first demonstration of a 212-kHz-linewidth single-frequency passively Q-switched EDFL using a few-layer Bi_2Se_3 SA. The modulation depth and the saturation intensity of the few-layer Bi_2Se_3 SA were measured to be ~5% and 1.8 MW/cm^2 at 1.56 μm, respectively. The SA triggered passive Q-switching of the EDFL, and a 1-m unpumped EDF together with a 0.06-nm-bandwidth fiber Bragg grating (FBG) acted as an ultra-narrow autotracking filter to ensure SLM operation. We therefore obtained the near-transform-limited Q-switched pulses with the time-bandwidth product of 0.53 (i.e., 212-kHz linewidth and 2.54-μs duration). Moreover, the SLM Q-switched pulses exhibited the optical spectral signal-to-noise ratio (SNR) as high as 62 dB and the radio-frequency (RF) SNR of 48 dB. This approach represents a new paradigm in low-noise, narrow-linewidth pulsed fiber laser sources for diverse applications in coherent detection and communications.

2. EXPERIMENTAL PREPARATION AND SETUP

A. Few-Layer Bi_2Se_3 Saturable Absorber

The few-layer Bi_2Se_3 used in our experiment was prepared by the liquid-phase exfoliation method described in Ref. [52]. As depicted in Fig. 1, the as-prepared Bi_2Se_3 nanosheets were characterized by transmission electron microscopy (TEM) and atomic force microscopy (AFM). Figure 1(a) gives the TEM image, in which the TI nanosheets exhibit the quasi-2D structure and have diameters from tens of nanometers to ~1 μm. Figures 1(b) and 1(c) give the typical AFM image and the corresponding height profile diagram, respectively. The average thickness was measured to be ~2–6 nm. Since the single-layer thickness of Bi_2Se_3 is 0.96 nm [64], the TI nanosheets prepared in our experiment have two to six layers.

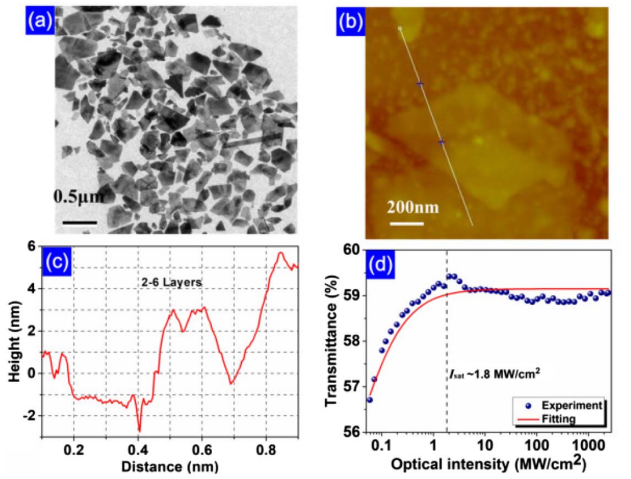

Fig. 1. Characterization of the as-prepared few-layer Bi_2Se_3. (a) TEM image, (b) AFM image, (c) height profile diagram, and (d) measured saturable absorption curve at 1.56 μm wavelength.

We measured the nonlinear saturable absorption characteristics of the few-layer Bi_2Se_3 nanosheets using a balanced twin-detector measurement system [27]. The measurement system consists of an amplified femtosecond fiber laser (center wavelength: 1566 nm; repetition rate: 8.54 MHz; pulse duration: 290 fs), a variable optical attenuator, a 3-dB optical coupler, and two power meters. As can be seen in Fig. 1(d), the optical transmission gradually increases and then remains almost constant, when the optical intensity on the few-layer Bi_2Se_3 polymer film increases. This shows a typical saturable absorption effect. Then, we numerically fitted the experimental data with the following formula:

$$T = 1 - \alpha_L - \Delta\alpha/(1 + I/I_{sat}). \quad (1)$$

Here, $\Delta\alpha$, I_{sat}, and α_L represent the modulation depth, saturation optical intensity, and the nonsaturable loss, respectively. The few-layer Bi_2Se_3 SA shows a saturation optical intensity (I_{sat}) of 1.8 MW/cm^2 and a modulation depth of ~5%. Considering that SLM laser operation usually restricts optical power intensity in a laser cavity, SAs with low saturable optical intensity and high modulation depth should be preferred; thus, the as-prepared few-layer Bi_2Se_3 SA could be ideal for SLM Q-switching.

B. Experimental Setup

Figure 2 shows the experimental setup of our proposed single-frequency passively Q-switched EDFL based on the Bi_2Se_3 SA. A 976-nm laser diode as a pump laser was coupled into the cavity by a 976/1550-nm wavelength division multiplexer. A section of 2.4-m EDF (Nufern EDFL-980-HP) with peak absorption ~18 dB/m at 976 nm was used as the gain medium. The as-prepared few-layer Bi_2Se_3 film as an SA was inserted into the cavity for initiating passive Q-switching. An optical circulator enforced the unidirectional laser operation. The combination of a ~1 m unpumped EDF (Nufern EDFL-980-HP) and narrow-linewidth FBG was designed to ensure the SLM operation (see Section 3.B for the principle explanation). The inset in Fig. 2 shows the transmission spectrum

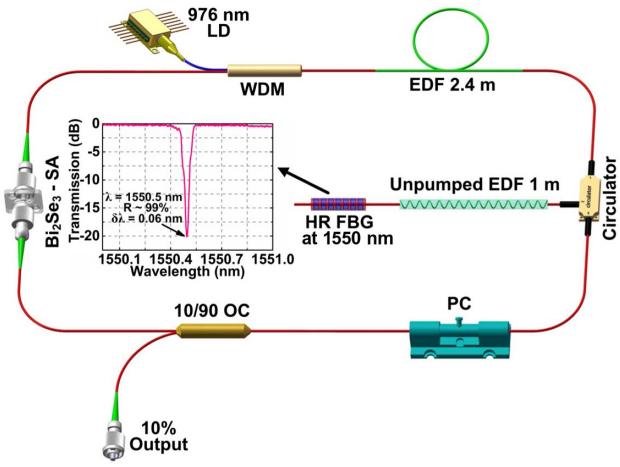

Fig. 2. Experiment setup of the proposed narrow-linewidth single-frequency passively *Q*-switched EDFL. WDM, wavelength division multiplexer; EDF, erbium-doped fiber; PC, polarization controller; OC, optical coupler. Inset: transmission spectrum of the narrow-bandwidth FBG.

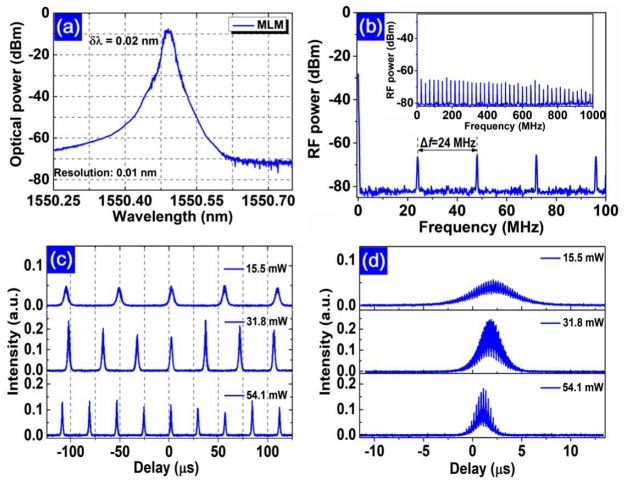

Fig. 3. MLM *Q*-switching characteristics. (a) Optical spectrum of the MLM *Q*-switched laser; (b) RF output spectrum of the MLM *Q*-switched laser in 100-MHz span (inset: 1-GHz span); (c) typical oscilloscope traces of the MLM *Q*-switched pulse trains; (d) single pulse envelope from the MLM *Q*-switched laser.

of the employed FBG, the center wavelength locates at 1550.5 nm with a high reflectivity of >99%, and the 3-dB bandwidth is as narrow as 0.06 nm. One can expect such an FBG will not only select the laser wavelength but also help to form the narrow-linewidth laser oscillation. The total cavity length is ~10.5 m, corresponding to ~20 MHz longitudinal mode spacing. In addition, an in-line fiber polarization controller was used to optimize laser operation, and the output power was extracted from the laser cavity through a 10/90 optical coupler.

3. EXPERIMENTAL RESULTS AND DISCUSSIONS

A. MLM *Q*-Switching

In order to clearly understand the performance differences between MLM and SLM *Q*-switching operation, at first, we investigated the MLM *Q*-switching without the 1-m unpumped EDF in the laser cavity. As we gradually increased the pump power, the 1.55-μm laser oscillation was observed at a threshold power of ~15.3 mW, and the passive *Q*-switching operation was initiated almost at the same time.

Figure 3(a) shows the optical spectrum of the *Q*-switching operation at the pump power of 54.1 mW. The center wavelength is 1550.49 nm, coinciding with the employed FBG. The 3-dB spectral bandwidth ($\delta\lambda$) is about 0.02 nm with a spectral resolution of 0.01 nm, corresponding to a frequency linewidth of 2.5 GHz. To further confirm the MLM oscillation, we then measured the RF output spectrum of the *Q*-switched laser, which obviously displays a chain of intermode-beating signals in either a 1-GHz wide span [inset in Fig. 3(b)] or a 100-MHz narrow span [Fig. 3(b)]. In addition, the longitudinal mode spacing (Δf) is 24 MHz, which coincides with the cavity round-trip frequency of the ~8.5 m cavity length (without the ~1 m unpumped EDF). Therefore, one can calculate that the 2.5-GHz linewidth of the *Q*-switched laser is comprised of ~104 longitudinal modes. Figure 3(c) depicts the typical oscilloscope traces of the *Q*-switched pulse trains under different pump powers. As the pump power is tuned from 15.5 mW to 54.1 mW, the pulse repetition rate monotonously increased from 18.7 kHz to 36.3 kHz, exhibiting the typical feature of passive *Q*-switching. The intensity fluctuation of the *Q*-switched pulses in Fig. 3(c) also indicates that the MLM *Q*-switching operation suffers a relatively poor stability, resulting from the mode turbulence among ~104 longitudinal modes. We further observed the fine structure in a single-pulse envelope from the *Q*-switched laser. As shown in Fig. 3(d), due to the strong self-mode-locking phenomenon in the MLM laser oscillation, one can clearly see that the *Q*-switching pulse contains lots of sub-pulse components inside.

B. SLM *Q*-Switching

For establishing the SLM *Q*-switching operation, the ~1 m unpumped EDF was then spliced between the circulator and the FBG, which together formed a linear standing wave arm [62]. The linear arm functions as a mode selector, in which two counter-propagating waves form a standing wave and induce spatial-hole-burning. Consequently, the refractive index of the unpumped EDF changes periodically and results in an ultranarrow-bandwidth self-induced FBG, which would cause very large losses at neighboring longitudinal modes and allow high transmission at the favored longitudinal mode [62,65]. Thus, the SLM lasing in our experiment could be established under the help of the self-induced FBG in the unpumped EDF. In this case, stable continuous-wave (CW) lasing at 1.55 μm was obtained at a slightly higher threshold of ~20 mW owing to the absorption loss induced by the unpumped EDF. However, the SLM *Q*-switching operation did not build up until the pump power was increased to ~98 mW. Figures 4(a) and 4(b) give the optical spectra at the pump power of 98 mW. As shown in Fig. 4(a), the SLM *Q*-switched laser with a center wavelength of 1550.50 nm exhibits a low-noise laser output

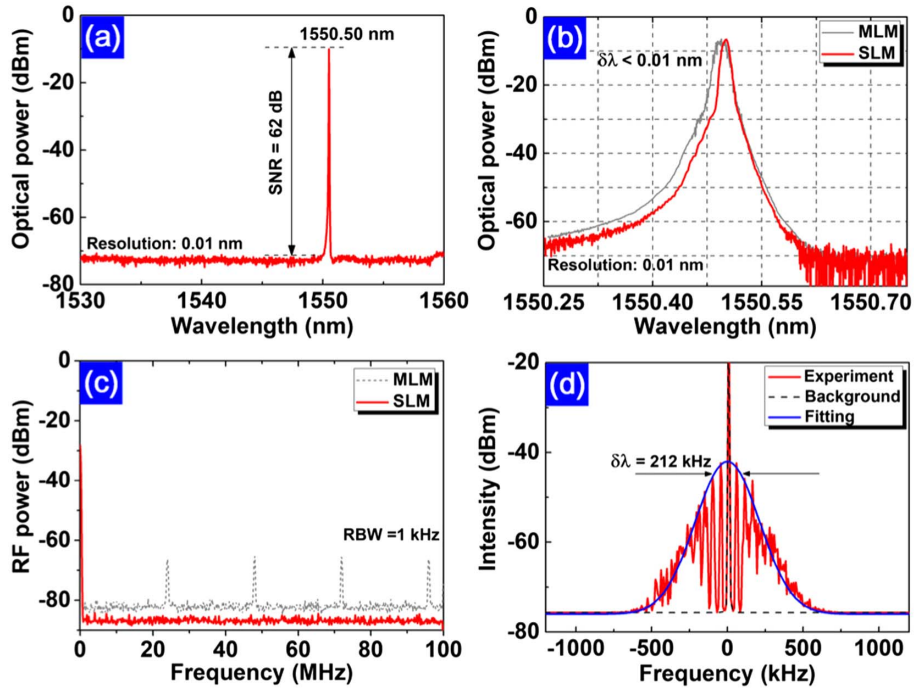

Fig. 4. SLM *Q*-switching characteristics. (a) Optical spectrum of the SLM *Q*-switched laser in a 30-nm span; (b) optical spectrum comparison of the SLM (red line) and the MLM (gray line) *Q*-switched lasers; (c) RF output spectrum comparison of the SLM (red solid line) and the MLM (gray dashed line) *Q*-switched lasers; (d) laser linewidth measurement with a resolution bandwidth (RBW) of 1 kHz by employing a self-heterodyne method; experimental data (red solid line), fitting (blue solid line), and equipment background (black dashed line).

with a high SNR of 62 dB, comparable to that of the conventional low-noise SLM Brillouin fiber lasers [66–68]. Figure 4(b) displays the SLM optical spectrum in a 0.5-nm span. Compared to the MLM operation (gray solid line), the SLM one (red solid line) shows a narrower linewidth. The real linewidth should be even narrower (<0.01 nm), limited by the resolution (0.01 nm) of our optical spectrum analyzer. The RF output spectrum was also recorded and compared in Fig. 4(c). Unlike the MLM operation that produces a series of intermode beating signals (gray dashed line), there appears no signal peak at this time (red solid line), confirming the stable SLM *Q*-switching operation. In our experiment, a self-heterodyne method at zero-frequency [69,70] with a 12-km-delayed fiber was employed to further measure the actual laser linewidth at the pump power of 98 mW. The experiment (red solid line), fitting (blue solid line), and equipment background (black dashed line) traces are shown in Fig. 4(d), respectively. The beat note forms a Gaussian lineshape by fitting the experimental data, and the 3-dB linewidth of the SLM *Q*-switched laser can be deduced to be 212 kHz [71].

To further clarify the SLM *Q*-switched characteristics, we observed the output pulse trains as shown in Fig. 5(a). With the increasing pump power, the repetition rate gradually increases. In contrast to the MLM operation, the SLM *Q*-switching pulses show a nearly uniform intensity and higher stability with the pulse-peak fluctuation <5%. Figure 5(b) plots the evolution of the single-pulse envelope under different pump powers. One can see that the pulse peak power monotonously increased with the pump power. Interestingly, there appears no sub-pulse in the *Q*-switching single pulse [unlike Fig. 3(d) in the MLM *Q*-switching case], thanks to the SLM operation, which is free of self-mode-locking effect. The inset in Fig. 5(b) shows the normalized-intensity single pulses, and the pulse duration becomes narrower when we increase the pump power.

We also measured the pulse repetition rate and the pulse duration as a function of the pump power. As shown in Fig. 5(c), when the pump power varied from 98 mW to 148 mW, the pulse repetition rate experienced a slight increase from 63.2 kHz to 68.9 kHz, and meanwhile the pulse duration gradually decreased from 2.54 μs to 1.49 μs. The slow increase of the repetition rate could be attributed to two reasons: (i) the SLM *Q*-switching initiated at a relatively high pump power of 98 mW, and thus the *Q*-switched laser always operated in a strong-pumping situation, i.e., high pumping rate; (ii) the Bi_2Se_3 SA always worked at the completed saturation state (i.e., operated at the maximum modulation depth) due to the high-power density in the SLM *Q*-switched cavity. Interestingly, considering the 212-kHz linewidth and the 2.54-μs pulse duration at the 98-mW pump power, the time-bandwidth product of the SLM *Q*-switched pulse was calculated to be ~0.53, which is very close to 0.44 for transform-limited Gaussian pulses. This is, to the best of our knowledge, the first SLM passively *Q*-switched fiber laser generating the transform-limited pulses.

To testify the stability of the SLM *Q*-switching operation, the RF spectrum under the pump power of 126 mW was recorded in Fig. 5(d) (narrow span) and its inset (wide span). The fundamental frequency centered at 65 kHz with the RF SNR of >48 dB, which is higher than that of the previous MLM *Q*-switching as well as most reported MLM *Q*-switched

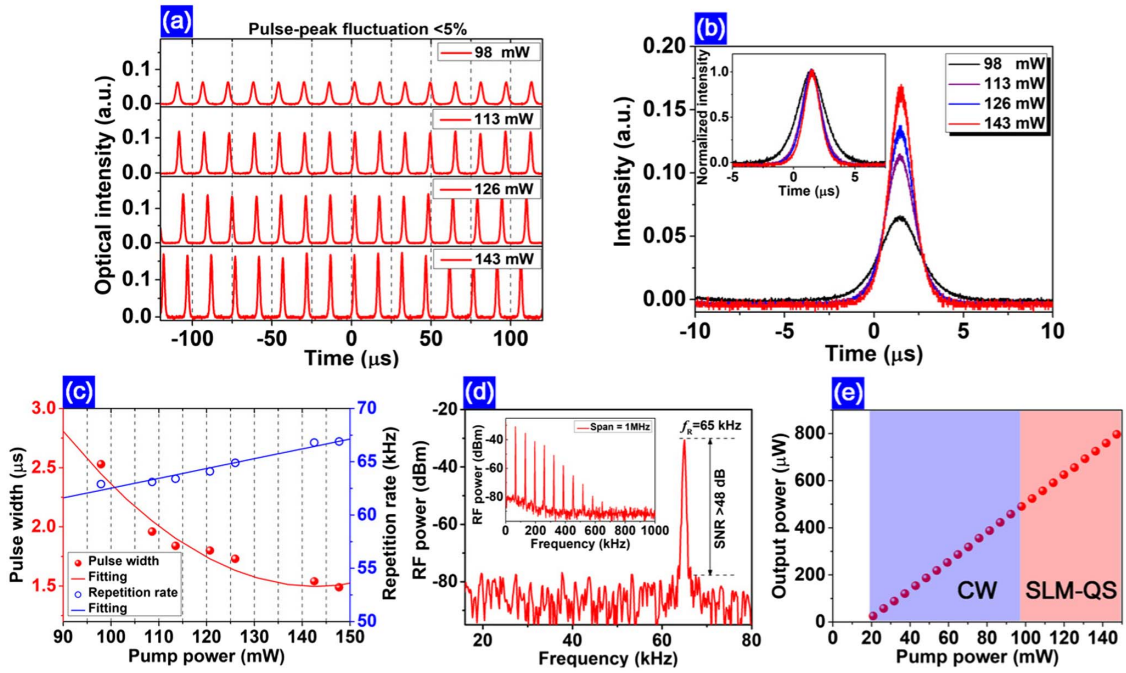

Fig. 5. (a) Typical oscilloscope traces of the SLM Q-switched pulse trains; (b) evolution of the single-pulse envelope; (c) repetition-rate and pulse duration as a function of the incident pump power; (d) RF output spectrum (inset: broadband RF output spectrum); (e) output power versus pump power.

fiber lasers [13,16–19]. The high RF SNR provides more evidence for the low-noise characteristic of our proposed SLM Q-switched fiber laser.

Finally, the average output power of the SLM Q-switched fiber laser was measured as a function of the pump power. One can see in Fig. 5(e) that there exist two different kinds of operation modes at different pump powers, which are the CW operation (pump power <98 mW) and the Q-switching operation (pump power >98 mW). As the pump power is increased, the average output power grows linearly without the appearance of saturation. The maximum output power obtained is 797 μW. When further increasing the pump power over 148 mW, we noticed in our experiment that the Q-switched pulse trains became unstable with strong amplitude fluctuation and even disappeared. The possible reason may be the over-bleaching of the Bi_2Se_3 SA at the high pumping strength.

4. CONCLUSION

In conclusion, 212-kHz-linewidth single-frequency, transform-limited pulses from the Q-switched EDFL based on a few-layer Bi_2Se_3 SA were proposed and experimentally demonstrated. The few-layer Bi_2Se_3 SA was used to initiate the Q-switching, while a 1-m unpumped EDF in combination with a narrow-bandwidth FBG was employed to achieve stable SLM operation at 1550.50 nm. Compared to the MLM Q-switching, the SLM one exhibits higher stability and lower noise. In our experiment, the SLM Q-switched pulses with the shortest pulse duration of 1.49 μs and the maximum output power of 797 μW were obtained. Our work may pave an effective way to achieve ultranarrow-linewidth, low-noise pulsed fiber lasers.

Funding. National Natural Science Foundation of China (NSFC) (61475129, 91750115); Fundamental Research Funds for the Central Universities (20720180057); Natural Science Foundation of Fujian Province (2017J06016); Program for New Century Excellent Talents in University (NCET) of Fujian Province, China.

Acknowledgment. The authors acknowledge Prof. Jian Weng from Department of Biomaterials, Xiamen University, for his help in the fabrication and characterization of the few-layer Bi_2Se_3.

REFERENCES

1. Z. Luo, M. Zhou, J. Weng, G. Huang, H. Xu, C. Ye, and Z. Cai, "Graphene-based passively Q-switched dual-wavelength erbium-doped fiber laser," Opt. Lett. **35**, 3709–3711 (2010).
2. C. Lee, Y. Chen, and S. Liaw, "Single-longitudinal-mode fiber laser with a passive multiple-ring cavity and its application for video transmission," Opt. Lett. **23**, 358–360 (1998).
3. O. Xu, S. Lu, S. Feng, Z. Tan, T. Ning, and S. Jian, "Single-longitudinal-mode erbium-doped fiber laser with the fiber-Bragg-grating-based asymmetric two-cavity structure," Opt. Commun. **282**, 962–965 (2009).
4. Y. Kaneda, Y. Hu, C. Spiegelberg, J. Geng, and S. Jiang, "Single-frequency, all-fiber Q-switched laser at 1550 nm," in *Advanced Solid-State Photonics*, Santa Fe, New Mexico (OSA, 2004), paper 126.
5. M. Laroche, A. M. Chardon, J. Nilsson, D. P. Shepherd, W. A. Clarkson, S. Girard, and R. Moncorgé, "Compact diode-pumped passively Q-switched tunable Er-Yb double-clad fiber laser," Opt. Lett. **27**, 1980–1982 (2002).
6. V. Philippov, A. Kir'yanov, and S. Unger, "Advanced configuration of erbium fiber passively Q-switched laser with Co^{2+}:ZnSe crystal as saturable absorber," IEEE Photon. Technol. Lett. **16**, 57–59 (2004).

7. R. Paschotta, R. Häring, E. Gini, H. Melchior, U. Keller, H. Offerhaus, and D. Richardson, "Passively *Q*-switched 0.1-mJ fiber laser system at 1.53 μm," Opt. Lett. **24**, 388–390 (1999).
8. J. Huang, W. Huang, W. Zhuang, K. Su, Y. Chen, and K. Huang, "High-pulse-energy, passively *Q*-switched Yb-doped fiber laser with AlGaInAs quantum wells as a saturable absorber," Opt. Lett. **34**, 2360–2362 (2009).
9. D. Zhou, L. Wei, B. Dong, and W. Liu, "Tunable passively *Q*-switched erbium-doped fiber laser with carbon nanotubes as a saturable absorber," IEEE Photon. Technol. Lett. **22**, 9–11 (2010).
10. H. Liu, K. Chow, S. Yamashita, and S. Set, "Carbon-nanotube-based passively *Q*-switched fiber laser for high energy pulse generation," Opt. Laser Technol. **45**, 713–716 (2013).
11. H. Zhang, D. Tang, R. Knize, L. Zhao, Q. Bao, and K. Loh, "Graphene mode locked, wavelength-tunable, dissipative soliton fiber laser," Appl. Phys. Lett. **96**, 111112 (2010).
12. A. Luo, P. Zhu, H. Liu, X. Zheng, N. Zhao, M. Liu, H. Cui, Z. Luo, and W. Xu, "Microfiber-based, highly nonlinear graphene saturable absorber for formation of versatile structural soliton molecules in a fiber laser," Opt. Express **22**, 27019–27025 (2014).
13. D. Popa, Z. Sun, T. Hasan, F. Torrisi, F. Wang, and A. Ferrari, "Graphene *Q*-switched, tunable fiber laser," Appl. Phys. Lett. **98**, 073106 (2011).
14. Z. Sun, T. Hasan, F. Torrisi, D. Popa, G. Privitera, F. Wang, F. Bonaccorso, D. Basko, and A. Ferrari, "Graphene mode-locked ultrafast laser," ACS Nano **4**, 803–810 (2010).
15. Q. Sheng, M. Feng, W. Xin, T. Han, Y. Liu, Z. Liu, and J. Tian, "Actively manipulation of operation states in passively pulsed fiber lasers by using graphene saturable absorber on microfiber," Opt. Express **21**, 14859–14866 (2013).
16. J. Liu, S. Wu, Q. Yang, and P. Wang, "Stable nanosecond pulse generation from a graphene-based passively *Q*-switched Yb-doped fiber laser," Opt. Lett. **36**, 4008–4010 (2011).
17. G. Xie, J. Ma, P. Lv, W. Gao, P. Yuan, L. Qian, H. Yu, H. Zhang, J. Wang, and D. Tang, "Graphene saturable absorber for *Q*-switching and mode locking at 2 μm wavelength [invited]," Opt. Mater. Express **2**, 878–883 (2012).
18. Y. Zhong, Z. Cai, D. Wu, Y. Cheng, J. Peng, J. Weng, Z. Luo, B. Xu, and H. Xu, "Passively *Q*-switched red Pr^{3+}-doped fiber laser with graphene-oxide saturable absorber," IEEE Photon. Technol. Lett. **28**, 1755–1758 (2016).
19. Y. Tang, X. Yu, X. Li, Z. Yan, and Q. Wang, "High-power thulium fiber laser *Q* switched with single-layer graphene," Opt. Lett. **39**, 614–617 (2014).
20. G. Zhu, X. Zhu, K. Balakrishnan, R. Norwood, and N. Peyghambarian, "Fe^{2+}:ZnSe and graphene *Q*-switched singly Ho^{3+}-doped ZBLAN fiber lasers at 3 μm," Opt. Mater. Express **3**, 1365–1377 (2013).
21. Z. Luo, M. Zhou, D. Wu, C. Ye, J. Weng, J. Dong, H. Xu, Z. Cai, and L. Chen, "Graphene-induced nonlinear four-wave-mixing and its application to multiwavelength *Q*-switched rare-earth-doped fiber lasers," J. Lightwave Technol. **29**, 2732–2739 (2011).
22. R. Woodward, R. Howe, G. Hu, F. Torrisi, M. Zhang, T. Hasan, and E. Kelleher, "Few-layer MoS_2 saturable absorbers for short-pulse laser technology: current status and future perspectives [invited]," Photon. Res. **3**, A30–A42 (2015).
23. A. Luo, M. Liu, X. Wang, Q. Ning, W. Xu, and Z. Luo, "Few-layer MoS_2-deposited microfiber as highly nonlinear photonic device for pulse shaping in a fiber laser [invited]," Photon. Res. **3**, A69–A78 (2015).
24. H. Xia, H. Li, C. Lan, C. Li, J. Du, S. Zhang, and Y. Liu, "Few-layer MoS_2 grown by chemical vapor deposition as a passive *Q*-switcher for tunable erbium-doped fiber lasers," Photon. Res. **3**, A92–A96 (2015).
25. Z. Luo, Y. Li, M. Zhong, Y. Huang, X. Wan, J. Peng, and J. Weng, "Nonlinear optical absorption of few-layer molybdenum diselenide ($MoSe_2$) for passively mode-locked soliton fiber laser [invited]," Photon. Res. **3**, A79–A86 (2015).
26. Y. Huang, Z. Luo, Y. Li, M. Zhong, B. Xu, K. Che, H. Xu, Z. Cai, J. Peng, and J. Weng, "Widely-tunable, passively *Q*-switched erbium-doped fiber laser with few-layer MoS_2 saturable absorber," Opt. Express **22**, 25258–25266 (2014).
27. Z. Luo, Y. Huang, M. Zhong, Y. Li, J. Wu, B. Xu, H. Xu, Z. Cai, J. Peng, and J. Weng, "1-, 1.5-, and 2-μm fiber lasers *Q*-switched by a broadband few-layer MoS_2 saturable absorber," J. Lightwave Technol. **32**, 4679–4686 (2014).
28. D. Mao, X. Cui, X. Gan, M. Li, W. Zhang, H. Lu, and J. Zhao, "Passively *Q*-switched and mode-locked fiber laser based on an ReS_2 saturable absorber," IEEE J. Sel. Top. Quantum Electron. **24**, 1100406 (2018).
29. M. Zhang, R. C. Howe, R. I. Woodward, E. J. Kelleher, F. Torrisi, G. Hu, S. V. Popov, J. R. Taylor, and T. Hasan, "Solution processed MoS_2-PVA composite for sub-bandgap mode-locking of a wideband tunable ultrafast Er:fiber laser," Nano Res. **8**, 1522–1534 (2015).
30. P. Yan, A. Liu, Y. Chen, H. Chen, S. Ruan, C. Guo, S. Chen, I. Li, H. Yang, J. Hu, and G. Cao, "Microfiber-based WS_2-film saturable absorber for ultra-fast photonics," Opt. Mater. Express **5**, 479–489 (2015).
31. H. Xia, H. Li, C. Lan, C. Li, X. Zhang, S. Zhang, and Y. Liu, "Ultrafast erbium-doped fiber laser mode-locked by a CVD-grown molybdenum disulfide (MoS_2) saturable absorber," Opt. Express **22**, 17341–17348 (2014).
32. J. Ren, S. Wang, Z. Cheng, H. Yu, H. Zhang, Y. Chen, L. Mei, and P. Wang, "Passively *Q*-switched nanosecond erbium-doped fiber laser with MoS_2 saturable absorber," Opt. Express **23**, 5607–5613 (2015).
33. D. Mao, X. She, B. Du, D. Yang, W. Zhang, K. Song, X. Cui, B. Jiang, T. Peng, and J. Zhao, "Erbium-doped fiber laser passively mode locked with few-layer WSe_2/$MoSe_2$ nanosheets," Sci. Rep. **6**, 23583 (2016).
34. J. Ma, S. Lu, Z. Guo, X. Xu, H. Zhang, D. Tang, and D. Fan, "Few-layer black phosphorus based saturable absorber mirror for pulsed solid-state lasers," Opt. Express **23**, 22643–22648 (2015).
35. S. Lu, Y. Ge, Z. Sun, Z. Huang, R. Cao, C. Zhao, S. Wen, D. Fan, J. Li, and H. Zhang, "Ultrafast nonlinear absorption and nonlinear refraction in few-layer oxidized black phosphorus," Photon. Res. **4**, 286–292 (2016).
36. Z. Luo, M. Liu, Z. Guo, X. Jiang, A. Luo, C. Zhao, X. Yu, W. Xu, and H. Zhang, "Microfiber-based few-layer black phosphorus saturable absorber for ultra-fast fiber laser," Opt. Express **23**, 20030–20039 (2015).
37. Z. Qin, G. Xie, H. Zhang, C. Zhao, P. Yuan, S. Wen, and L. Qian, "Black phosphorus as saturable absorber for the *Q*-switched Er:ZBLAN fiber laser at 2.8 μm," Opt. Express **23**, 24713–24718 (2015).
38. X. Jin, G. Hu, M. Zhang, Y. Hu, T. Albrow-Owen, R. C. T. Howe, T.-C. Wu, Q. Wu, Z. Zheng, and T. Hasan, "102 fs pulse generation from a long-term stable, inkjet-printed black phosphorus-mode-locked fiber laser," Opt. Express **26**, 12506–12513 (2018).
39. Y. Chen, S. Chen, J. Liu, Y. Gao, and W. Zhang, "Sub-300 femtosecond soliton tunable fiber laser with all-anomalous dispersion passively mode locked by black phosphorus," Opt. Express **24**, 13316–13324 (2016).
40. H. Yu, X. Zheng, K. Yin, X. Cheng, and T. Jiang, "Nanosecond passively *Q*-switched thulium/holmium-doped fiber laser based on black phosphorus nanoplatelets," Opt. Mater. Express **6**, 603–609 (2016).
41. X. Jiang, S. Liu, W. Liang, S. Luo, Z. He, Y. Ge, H. Wang, R. Cao, F. Zhang, Q. Wen, J. Li, Q. Bao, D. Fan, and H. Zhang, "Broadband nonlinear photonics in few-layer MXene $Ti_3C_2T_x$ (T = F, O, or OH)," Laser Photon. Rev. **12**, 1700229 (2017).
42. X. Jiang, X. Jiang, L. Zhang, S. Liu, Y. Zhang, Z. He, W. Li, F. Zhang, Y. Shi, W. Lü, Y. Li, Q. Wen, J. Li, J. Feng, S. Ruan, Y. Zeng, X. Zhu, Y. Lu, and H. Zhang, "Ultrathin metal-organic framework: an emerging broadband nonlinear optical material for ultrafast photonics," Adv. Opt. Mater. **2018**, 1800561 (2018).
43. X. Jiang, S. Gross, H. Zhang, Z. Guo, M. Withford, and A. Fuerbach, "Bismuth telluride topological insulator nanosheet saturable absorbers for *Q*-switched mode-locked Tm:ZBLAN waveguide lasers," Ann. Phys. **528**, 543–550 (2016).
44. C. Zhao, Y. Zou, Y. Chen, Z. Wang, S. Lu, H. Zhang, S. Wen, and D. Tang, "Wavelength-tunable picosecond soliton fiber laser with topological insulator: Bi_2Se_3 as a mode locker," Opt. Express **20**, 27888–27895 (2012).

45. C. Zhao, H. Zhang, X. Qi, Y. Chen, Z. Wang, S. Wen, and D. Tang, "Ultra-short pulse generation by a topological insulator based saturable absorber," Appl. Phys. Lett. **101**, 211106 (2012).
46. Y. Chen, C. Zhao, H. Huang, S. Chen, P. Tang, Z. Wang, S. Lu, H. Zhang, S. Wen, and D. Tang, "Self-assembled topological insulator: Bi_2Se_3 membrane as a passive *Q*-switcher in an erbium-doped fiber laser," J. Lightwave Technol. **31**, 2857–2863 (2013).
47. Y. Chen, C. Zhao, S. Chen, J. Du, P. Tang, G. Jiang, H. Zhang, S. Wen, and D. Tang, "Large energy, wavelength widely tunable, topological insulator *Q*-switched erbium-doped fiber laser," IEEE J. Sel. Top. Quantum Electron. **20**, 315–322 (2014).
48. Z. Luo, M. Liu, H. Liu, X. Zheng, A. Luo, C. Zhao, H. Zhang, S. Wen, and W. Xu, "2 GHz passively harmonic mode-locked fiber laser by a microfiber-based topological insulator saturable absorber," Opt. Lett. **38**, 5212–5215 (2013).
49. M. Jung, J. Lee, J. Koo, J. Park, Y. Song, K. Lee, S. Lee, and J. Lee, "A femtosecond pulse fiber laser at 1935 nm using a bulk-structured Bi_2Se_3 topological insulator," Opt. Express **22**, 7865–7874 (2014).
50. Z. Yu, Y. Song, J. Tian, Z. Dou, H. Guoyu, K. Li, H. Li, and X. Zhang, "High-repetition-rate *Q*-switched fiber laser with high quality topological insulator Bi_2Se_3 film," Opt. Express **22**, 11508–11515 (2014).
51. D. Wu, Z. Cai, Y. Zhong, J. Peng, J. Weng, Z. Luo, N. Chen, and H. Xu, "635-nm visible Pr^{3+}-doped ZBLAN fiber lasers *Q*-switched by topological insulators SAs," IEEE Photon. Technol. Lett. **27**, 2379–2382 (2015).
52. Z. Luo, Y. Huang, J. Weng, H. Cheng, Z. Lin, B. Xu, Z. Cai, and H. Xu, "1.06 μm *Q*-switched ytterbium-doped fiber laser using few-layer topological insulator Bi_2Se_3 as a saturable absorber," Opt. Express **21**, 29516–29522 (2013).
53. Z. Luo, C. Liu, Y. Huang, D. Wu, J. Wu, H. Xu, Z. Cai, Z. Lin, L. Sun, and J. Weng, "Topological-insulator passively *Q*-switched double-clad fiber laser at 2 μm wavelength," IEEE J. Sel. Top. Quantum Electron. **20**, 0902708 (2014).
54. J. Li, H. Luo, L. Wang, C. Zhao, H. Zhang, H. Li, and Y. Liu, "3-μm mid-infrared pulse generation using topological insulator as the saturable absorber," Opt. Lett. **40**, 3659–3662 (2015).
55. W. Liu, L. Pang, H. Han, W. Tian, H. Chen, M. Lei, P. Yan, and Z. Wei, "70-fs mode-locked erbium-doped fiber laser with topological insulator," Sci. Rep. **6**, 19997 (2016).
56. M. Wu, Y. Chen, H. Zhang, and S. Wen, "Nanosecond *Q*-switched erbium-doped fiber laser with wide pulse-repetition-rate range based on topological insulator," IEEE J. Quantum Electron. **50**, 393–396 (2014).
57. J. Sotor, G. Sobon, and K. M. Abramski, "Sub-130 fs mode-locked Er-doped fiber laser based on topological insulator," Opt. Express **22**, 13244–13249 (2014).
58. P. Yan, R. Lin, H. Chen, H. Zhang, A. Liu, H. Yang, and S. Ruan, "Topological insulator solution filled in photonic crystal fiber for passive mode-locked fiber laser," IEEE Photon. Technol. Lett. **27**, 264–267 (2015).
59. Y. Chen, M. Wu, P. Tang, S. Chen, J. Du, G. Jiang, Y. Li, C. Zhao, H. Zhang, and S. Wen, "The formation of various multi-soliton patterns and noise-like pulse in a fiber laser passively mode-locked by a topological insulator based saturable absorber," Laser Phys. Lett. **11**, 055101 (2014).
60. P. Tang, M. Wu, Q. Wang, L. Miao, B. Huang, J. Liu, C. Zhao, and S. Wen, "2.8-μm pulsed Er^{3+}: ZBLAN fiber laser modulated by topological insulator," IEEE Photon. Technol. Lett. **28**, 1573–1576 (2016).
61. Y. I. Jhon, J. Lee, Y. M. Jhon, and J. H. Lee, "Topological insulators for mode-locking of 2-μm fiber lasers," IEEE J. Sel. Top. Quantum Electron. **24**, 1102208 (2018).
62. K. Zhang and J. U. Kang, "C-band wavelength-swept single-longitudinal-mode erbium-doped fiber ring laser," Opt. Express **16**, 14173–14179 (2008).
63. C. H. Yeh, T. T. Huang, H. C. Chien, C. H. Ko, and S. Chi, "Tunable S-band erbium-doped triple-ring laser with single-longitudinal-mode operation," Opt. Express **15**, 382–386 (2007).
64. N. Bansal, Y. S. Kim, E. Edrey, M. Brahlek, Y. Horibe, K. Iida, M. Tanimura, G. H. Li, T. Feng, H. D. Lee, T. Gustafsson, E. Andrei, and S. Oh, "Epitaxial growth of topological insulator Bi_2Se_3 film on Si(111) with atomically sharp interface," Thin Solid Films **520**, 224–229 (2011).
65. N. J. C. Libatique, L. Wang, and R. K. Jain, "Single-longitudinal-mode tunable WDM-channel-selectable fiber laser," Opt. Express **10**, 1503–1507 (2002).
66. S. Norcia, S. Tonda-Goldstein, D. Dolfi, J. P. Huignard, and R. Frey, "Efficient single-mode Brillouin fiber laser for low-noise optical carrier reduction of microwave signals," Opt. Lett. **28**, 1888–1890 (2003).
67. K. S. Abedin, P. S. Westbrook, J. W. Nicholson, J. Porque, T. Kremp, and X. Liu, "Single-frequency Brillouin distributed feedback fiber laser," Opt. Lett. **37**, 605–607 (2012).
68. G. Wang, L. Zhan, J. Liu, T. Zhang, J. Li, L. Zhang, J. Peng, and L. Yi, "Watt-level ultrahigh-optical signal-to-noise ratio single-longitudinal-mode tunable Brillouin fiber laser," Opt. Lett. **38**, 19–21 (2013).
69. C. Guo, K. Che, H. Xu, P. Zhang, D. Tang, C. Ren, Z. Luo, and Z. Cai, "Generation of optical frequency combs in a fiber-ring/microresonator laser system," Opt. Lett. **41**, 2576–2579 (2016).
70. L. Richter, H. Mandelberg, M. Kruger, and P. McGrath, "Linewidth determination from self-heterodyne measurements with subcoherence delay times," IEEE J. Quantum Electron. **22**, 2070–2074 (1986).
71. H. Ludvigsen, M. Tossavainen, and M. Kaivola, "Laser linewidth measurements using self-homodyne detection with short delay," Opt. Commun. **155**, 180–186 (1998).